Catalysis Today 175 (2011) 231–237

Contents lists available at ScienceDirect

Catalysis Today

journal homepage: www.elsevier.com/locate/cattod

Gold versus platinum on ceria–zirconia mixed oxides in oxidation of ethanol and toluene

J. Gaálová*, P. Topka, L. Kaluža, O. Šolcová

Institute of Chemical Process Fundamentals of the ASCR, v. v. i., Rozvojová 135, 165 02 Prague 6, Czech Republic

ARTICLE INFO

Article history:
Received 14 October 2010
Received in revised form 30 April 2011
Accepted 16 May 2011
Available online 17 June 2011

Keywords:
Gold
Platinum
Cerium
Zirconium
Oxidation
Ethanol
Toluene

ABSTRACT

The Ce–Zr mixed oxides have been examined as supports for platinum and gold in oxidation of ethanol and toluene. A weight ratio of Ce/Zr in the synthesized supports was 1/1. Two supported noble metals with a different loading (2.5 and 0.3 wt.%) were compared to each other as well as to selected industrial catalysts (HHC-5557 and VOC-1544). Whatever the metal content was, Pt catalysts were always more active in oxidation of ethanol and toluene than Au catalysts. Better reductive capability of platinum was confirmed by H_2-TPR profiles and a higher activity of platinum may also be linked to changes in surface basic properties (a higher amount of basic centers) illustrated by CO_2-TPD profiles. Deposition of gold on Ce–Zr mixed oxide resulted in a formation of certain amounts of crystalline Au phase detected by X-ray diffraction while the deposition of platinum did not produce any crystalline Pt phase. As observed by FE-SEM, part of Au was well dispersed but significant amount of Au was present as inactive crystals. Platinum catalysts were comparable or even more active than industrial catalysts (50% conversion of ethanol was achieved with 2.5Pt/CeZr(1) at 99 °C). On the other hand, gold catalysts proved the best selectivity in oxidation of ethanol.

1. Introduction

Volatile organic compounds (VOCs) are emitted into the atmosphere from thousands of sources and may have short and long-term adverse health effects. They are widely used as ingredients in household products or fuels made up of organic chemicals; all of these products can release organic compounds while they are used, and, to some degree, when they are stored [1].

In our work, we focus on two compounds: ethanol and toluene. Toluene is classified as VOC and it is a model aromatic hydrocarbon. Ethanol was chosen intentionally to focus on the emerging environmental problems of nowadays such as E-85 combustion (linked to the rising biofuel production), which actually augments the output of two different carcinogens, namely formaldehyde and acetaldehyde.

Catalytic oxidation of VOCs can be effectively applied to remove air pollutants from tail gases of industrial processes [2]. Employing the suitable catalysts for ethanol or toluene oxidation to CO_2 and H_2O requires significantly lower temperatures than those needed in thermal oxidation [3,4] besides, the use of the appropriate catalytic material avoids generation of dangerous reaction by-products [5].

Noble metal catalysts are generally favourable because of their high activity. Those materials are very stable and indicate the advantage of good selectivity to form CO_2 [6]. From different noble metals, platinum is often present as a part of the most active catalysts in oxidation of toluene [7–21] and ethanol [22–33]. Gold is less exploited in oxidation of both molecules [34–36,8,10,37–41]. With the view of better dispersion and mechanical resistance, the metals are usually supported by appropriate materials. In the 1990s, many studies were devoted to ceria-based materials, notably to their synthesis and their catalytic properties, e.g., they were used as structural and electronic promoters to increase the activity, selectivity and thermal stability of catalysts [42–45]. CeO_2–ZrO_2 oxides demonstrate the unique combination of an elevated oxygen transport capacity coupled with the ability to shift easily between reduced and oxidized state Ce^{3+}–Ce^{4+}. It induces a high refilling of active oxygen at the catalyst surface. Their success in the field of catalysis is mainly due to this high oxygen mobility and oxygen storage capacity (OSC) [46–48]. Recently, Ce–Zr mixed oxides were proposed as catalysts for the oxidation of VOCs [49,50].

The aim of this work was to examine the possibility of using Ce–Zr mixed oxides as supports for two noble metals, particularly active in oxidation of volatile organic compounds, gold and

* Corresponding author. Tel.: +420 220 390 282; fax: +420 220 920 661.
E-mail address: gaalova@icpf.cas.cz (J. Gaálová).

0920-5861/$ – see front matter © 2011 Elsevier B.V. All rights reserved.
doi:10.1016/j.cattod.2011.05.011

platinum. New Pt and Au catalysts were prepared, characterized and tested in total oxidation of ethanol and toluene.

2. Experimental

2.1. Catalyst preparation

After dissolution of 38 g of zirconium n-propoxide (70 wt.% solution in propan-1-ol, Fluka, prod. No. 96595) in 51 mL of propan-2-ol (Lach-Ner, prod. No. 30470), the solution was added to the solution of 25 g of cerium(III) nitrate hexahydrate (Strem Chemicals, prod. No. 93-5831) in 25 mL distilled water with a rate of 5 mL min^{-1} under vigorous stirring at ambient temperature. A pseudogel was formed immediately as the reactant hydrolyzed. The pseudogel was dried either overnight at ambient temperature (batch 1) or over a sand bath at 60 °C for 1 h (batch 2). Then the samples were dried in an oven at 120 °C for 24 h and calcined in a batch furnace at 500 °C with a temperature ramp rate 5 °C min^{-1} and dwell time 1 h at 300 °C and 5 h at 500 °C. The samples were then crushed and sieved to particle size fraction 0.16–0.32 mm and labelled CeZr(1) and CeZr(2), respectively.

3 g of the supports CeZr(1) and CeZr(2) were impregnated with 6 mL of aqueous solutions of either gold(III) acetate (Alfa Aesar, prod. No. 39742) or platinum(II) tetraaminehydroxide (Alfa Aesar, prod. No. 42918) in rotary vacuum evaporator at 30 °C in order to deposit 2.5 and 0.3 wt.% of the metals. The samples were dried in an oven at 120 °C for 24 h and labelled 0.3Au/CeZr(1), 2.5Au/CeZr(1), 0.3Au/CeZr(2), 2.5Au/CeZr(2), 0.3Pt/CeZr(1), 2.5Pt/CeZr(1), 0.3Pt/CeZr(2), and 2.5Pt/CeZr(2). Prepared catalysts were compared to two industrial catalysts supported on alumina: HHC-5557 (0.13 wt.% Pt, 0.04 wt.% Pd) and VOC-1544 (3.34 wt.% Cu, 5.44 wt.% Mn) that were purchased from Südchemie.

2.2. Characterization

The prepared samples were characterized by chemical analysis (ICP), thermogravimetric analysis, powder X-ray diffraction (XRD), N_2 physisorption, temperature programmed techniques (TPR, TPD) and field-emission scanning electron microscopy (FE-SEM).

Chemical analysis of samples was performed on the ICP OES instrument Intrepid II DUO and GBC Avanta instrument. The concentration of elements was quantified in solutions obtained after decomposition of samples by melting in $KHSO_4$ in porcelain crucibles, filtration and dissolution in water.

Thermogravimetric analysis of the supports dried at 120 °C and/or calcined was done in air with a temperature ramp rate of 10 °C min^{-1} to 900 °C using thermobalance Stanton-Redcroft TG-750.

The X-ray diffraction data were collected on a Philips X'Pert MPD system in Bragg–Brentano geometry using CuKα radiation and a secondary graphite monochromator in the range of 10–80° 2 theta at a rate of measurement of 0.02° s^{-1}. The size of CeO_2–ZrO_2 and Au crystallites was calculated from the Scherrer equation.

N_2 physisorption was performed with Micromeritics ASAP 2010, after drying the samples at 105 °C for 24 h and evacuation at 350 °C until the pressure 10^{-5} Pa was achieved (usually 2–5 h). The adsorption–desorption isotherms of nitrogen at −195 °C were treated by the standard Brunauer–Emmett–Teller (BET) procedure to calculate the specific surface area S_{BET}. The total volume of pores V_P was calculated from the amount of N_2 adsorbed at $P/P_o = 0.98$. The surface area of mesopores S_M and the volume of micropores V_{Micro} were determined by *t*-plot method. Pore size distribution was calculated from the desorption branch of the adsorption–desorption isotherm by the Barrett–Joyner–Halenda (BJH) method.

Temperature-programmed reduction (TPR) measurements of the calcined samples (0.025 g) were performed with a H_2/N_2 mixture (10 mol% H_2), flow rate 50 mL min^{-1} and linear temperature increase 20 °C min^{-1} up to 1000 °C. A change in H_2 concentration was detected with a mass spectrometer Omnistar 300 (Pfeiffer Vacuum). Reduction of the grained CuO (0.16–0.315 mm) was repeatedly performed to calculate absolute values of hydrogen consumed during reduction.

Temperature-programmed desorption (TPD) of NH_3 and CO_2 was carried out to examine acid and basic properties of the catalysts surface, respectively. The measurements were accomplished with 0.050 g of a sample in the temperature range 20–1000 °C, with helium as a carrier gas and CO_2 or NH_3 as adsorbing gases. The heating rate 20 °C min^{-1} was applied. During the experiments the following mass contributions m/z were collected: 2-H_2, 18-H_2O, 16-NH_3, and 44-CO_2. The spectrometer was calibrated by dosing an amount (840 μl) of CO_2 or NH_3 into the carrier gas (He) in every experiment. The TPR and TPD experiments were evaluated using OriginPro 7.5 software with an accuracy of ±5%.

Field-emission scanning electron microscopy (FE-SEM) images were taken using JSM-6700F scanning electron microscope. The samples for FE-SEM measurements were prepared by depositing the powder sample on a graphite drop.

2.3. Catalytic experiments

Catalytic reaction was carried out in a fixed-bed glass reactor (5 mm i.d.) in the temperature range from 50 to 400 °C (the temperature of the furnace was linearly increased with the rate of 2 °C min^{-1}). The catalyst (0.4 g of sieved grains with particle size of 0.16–0.315 mm) was examined at 20 m^3 kg^{-1} h^{-1} space velocity (GHSV). The inlet concentration of model compounds (MC) in the air was 1 g m^{-3} (toluene and ethanol were chosen as MC). Reaction products were analyzed using a gas chromatograph Hewlett-Packard 6890 equipped with a FID detector and a capillary column (HP-5 19091 J-413, 30 m × 0.32 mm × 0.25 mm with 5% phenylmethyl silicone). The concentrations of CO and CO_2 were monitored using a Siemens Ultramat 23 infrared analyzer. Conversion of the examined MC *C* and selectivity to carbon dioxide *S* were calculated based on the material balance using Eqs. (1) and (2):

$$C = \frac{a_{MC}^{in} - a_{MC}}{a_{MC}^{in}} \quad (1)$$

$$S = \frac{n(a_{MC}^{in} - a_{MC}/f_{MC}M_{MC}) - \sum(n_i a_i / f_i M_i)}{n(a_{MC}^{in} - a_{MC}/f_{MC}M_{MC}) - \sum((n_i - 1)a_i / f_i M_i)} \quad (2)$$

where a_{MC}^{in} is the GC peak area of the examined MC corresponding to its inlet concentration (1 g m^{-3}), a_{MC} is the GC peak area of the examined MC, n is the number of carbon atoms in the molecule of examined MC, f_{MC} is experimentally determined FID relative response factor of examined MC (1.18 for ethanol and 1.05 for toluene), M_{MC} is the molecular weight of the examined MC, n_i is the number of carbon atoms in the molecule of corresponding by-product, a_i is the GC peak area of corresponding by-product, f_i is experimentally determined FID relative response factor of corresponding by-product (1.00 for ethylene and 0.50 for acetaldehyde), and M_i is the molecular weight of corresponding by-product. The accuracy of the conversion and selectivity determination was ±2%. Temperatures T_{50} and T_{90} (the temperature at which 50 and 90% conversion of the examined MC was observed, respectively) were chosen as a measure of catalyst activity. The selectivity of the catalysts was evaluated as the selectivity to CO_2 at 95% conversion of the examined MC (S_{95}). In order to eliminate the influence of

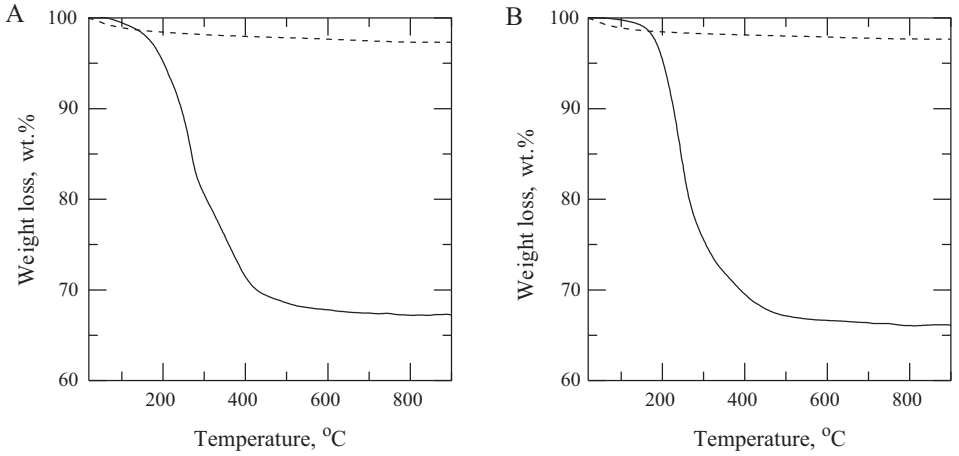

Fig. 1. (A) Solid line – CeZr(1) dried at 120 °C, dashed line CeZr(1) calcined at 500 °C; (B) solid line – CeZr(2) dried at 120 °C, dashed line CeZr(2) calcined at 500 °C.

CO_2 adsorption on the catalyst, the selectivity was computed from GC peak areas using material balance according to Eq. (2); at 95% conversion, the presence of CO was not detected in any of the experiments.

3. Results and discussion

3.1. Characterization

Chemical analysis confirmed that the weight ratio of Ce/Zr in the synthesized supports was close to 1/1 (1.01–1.15/1). The actual loadings of Au and Pt in the selected catalysts 0.3Au/CeZr(2), 2.5Au/CeZr(2), 0.3Pt/CeZr(2), and 2.5Pt/CeZr(2) were found to be 0.3, 2.8, 0.2, and 1.5 wt.%, respectively. Bearing in mind measurement uncertainty of the chemical analysis (20%) and operation with low amount of sample (potential inhomogeneity), the impregnation method deposited the precious metals onto the support quite successfully.

Thermogravimetric analysis of the support studied is shown if Fig. 1. It is seen that the supports dried at 120 °C lost about 25 wt.% between 200 and 400 °C. For that reason the samples were kept at 300 °C for 1 h prior to further temperature increase to 500 °C during the preparation procedure. The calcined supports exhibited only about 2.5 wt.% loss during the thermogravimetrical analysis, which confirmed the stability of the supports. This low weight loss could

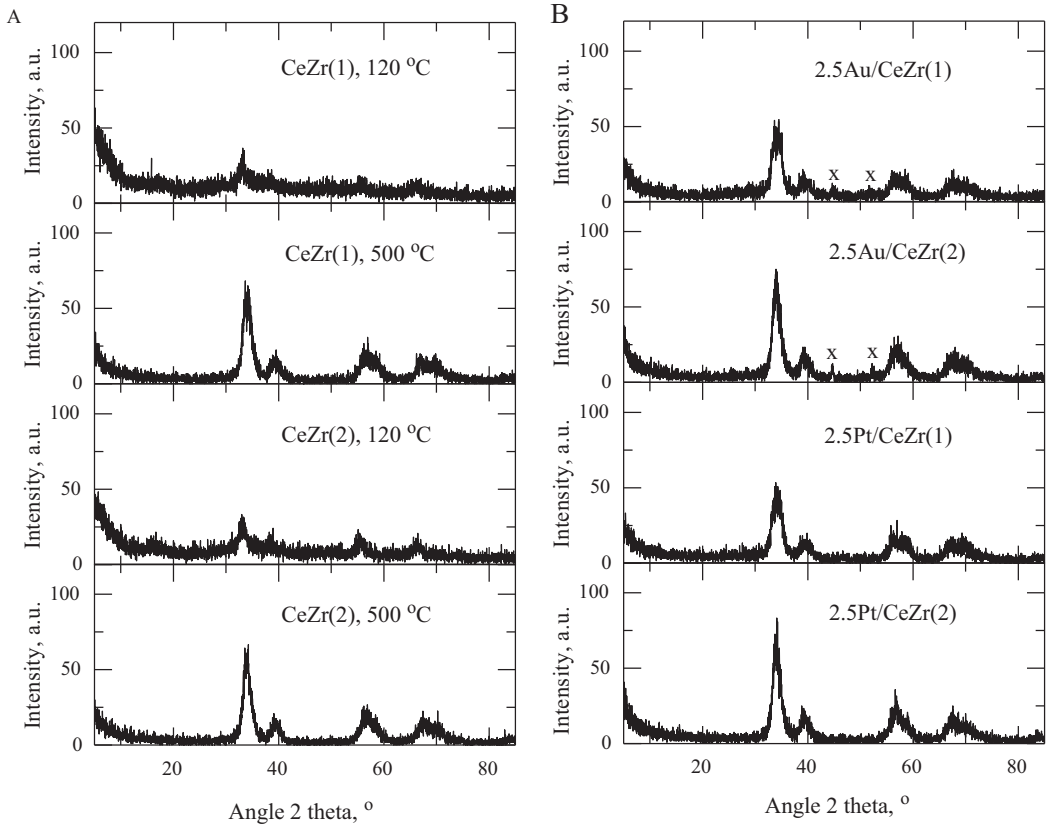

Fig. 2. X-ray diffraction patterns. (A) The supports CeZr(1) and CeZr(2) dried at 120 °C or calcined at 500 °C; (B) the selected catalysts calcined at 500 °C, x – peaks of crystalline Au.

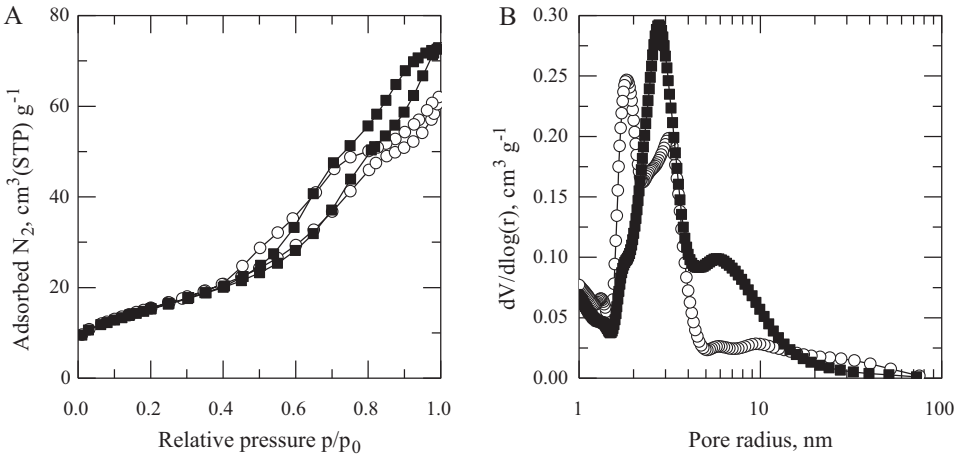

Fig. 3. (A) N_2 adsorption–desorption isotherms. (B) Pore-size distributions. CeZr(1) – open circle; CeZr(2) – filled squares.

be ascribed to physically bounded water in porous systems of the supports. It was concluded that both batches CeZr(1) and CeZr(2) did not differ in thermogravimetrical analysis.

X-ray diffraction patterns of the supports and selected catalysts are shown in Fig. 2 together with the effect of calcination. It was found that the crystalline phase was already formed after the drying of the supports CeZr(1) and CeZr(2) at 120 °C showing the crystallite size to be about 10 and 9 nm. Calcination, however, significantly extended the crystallization. The patterns are consistent with the patterns presented in literature [51,52]. Furthermore, differences between the preparation procedure of the support CeZr(1) and CeZr(2) (drying overnight at ambient temperature and drying on a sand bath at 60 °C) did not affect the resulting crystalline size, which remained low (about 9 nm). Deposition of gold resulted in a formation of certain amounts of crystalline Au phase (Au crystallite size was about 44 and 37 nm for 2.5Au/CeZr(1) and 2.5Au/CeZr(2), respectively) while the deposition of platinum did not produce crystalline Pt phase.

N_2 physisorption was employed to determine the textural parameters of the supports and selected catalysts. The results are summarized in Table 1. Nitrogen adsorption-desorption isotherms and pore-size distribution are shown in Fig. 3. It is seen that the supports exhibited similar adsorption–desorption isotherms and textural parameters while the pore-size distribution slightly differed. The bimodal porous systems with main maxima centered about 2.8 and 6 nm for CeZr(1) and CeZr(2) respectively were more pronounced over CeZr(2) than over CeZr(1). Moreover, the maximum at 1.8 nm was not pronounced over CeZr(2) support. CeZr(2), furthermore, exhibited 1.25 times higher total pore volume V_P than CeZr(1).

Reducibility of the mixed oxide and selected catalysts was examined by temperature-programmed reduction using hydrogen as a reductant. Fig. 4 demonstrates distinct differences between the bare support and metal containing catalysts. The TPR profile of support CeZr(1) (Fig. 4C) showed reduction peak maxima at temperatures close to 480 and 700 °C. A lower temperature signal located at 480 °C was assigned to the reduction of the surface, while the reduction of the bulk was responsible for the high-temperature signal at 700 °C. In contrast, the TPR profiles of noble metal catalysts essentially showed a main broad reduction feature at significantly lower temperatures: between 200 and 420 °C for Au catalysts while for Pt samples already between 110 and 400 °C. The shift toward the lower temperature is more pronounced for the catalysts with higher loading (2.5 wt.%). This indicates the promotion of Ce^{4+} reduction. It can be related to enhancement of mobility and diffusion of bulk O_2 due to the metal addition. As we know, the peak area has a direct correlation with the amount of reductive species. When the area of the peak is bigger, there is a higher amount of reductive species and a stronger reductive capability. Compared with the support CeZr(1), Au catalysts and even more Pt catalysts have a bigger peak area, which demonstrates that noble metal has a positive effect on reductive capability for CeZr(1) [53].

From the TPD patterns of NH_3 (Fig. 5), two peaks were identified for both the bare support and the metal catalysts. They correspond to weak (T_{max} around 125 °C) and strong (T_{max} around 307 °C) acid centers. The high-temperature peak (representing acid centers of high strength) of the catalyst containing gold was slightly shifted to a lower temperature while its low-temperature peak (representing acid centers of low strength) was slightly shifted to a higher temperature. Considering a low amount of metal (0.3 wt.%) introduced on the examined support, gold addition caused certain decrease of amount of strong acid centers and small increase of amount of weak acid centers. TPD of CO_2 for three selected catalysts (Fig. 6) visualized changes in surface basic properties related to the impregnation of noble metals. The peak at about 94 °C corresponds to basic centers of moderate strength. Comparing to CeZr(1) (Fig. 6A), gold catalyst (Fig. 6B) and even more platinum catalyst (Fig. 6C) indicate a shift of a peak maximum to higher temperatures. It means that addition of gold and especially addition of platinum increases the strength of basic centers of the support. A higher area of the peak for

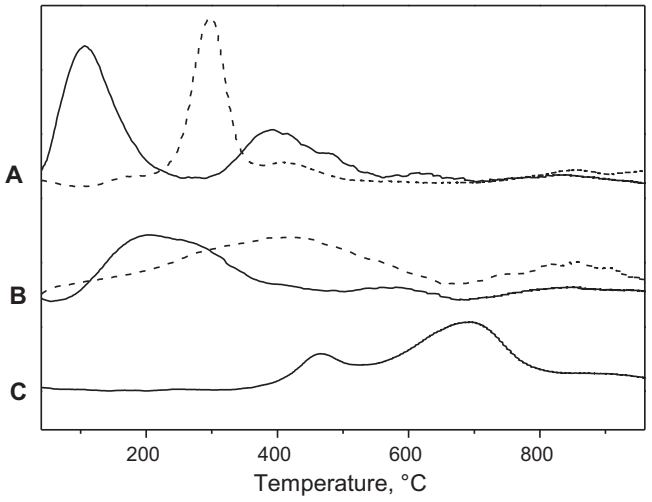

Fig. 4. H_2-TPR profiles of (A) solid line – 2.5Pt/CeZr(1), dashed line – 0.3Pt/CeZr(1), (B) solid line – 2.5Au/CeZr(1), dashed line – 0.3Au/CeZr(1) and (C) support CeZr(1).

Table 1
Textural parameters of the supports.

	Specific surface area, S_{BET} ($m^2\ g^{-1}$)	Total pore volume, V_P ($mm^3\ g^{-1}$)	Mesopore surface area, S_M ($m^2\ g^{-1}$)	Micropore volume, V_{Micro} ($cm^3\ g^{-1}$)
CeZr(1)	56	88	37	14
CeZr(2)	55	110	35	14

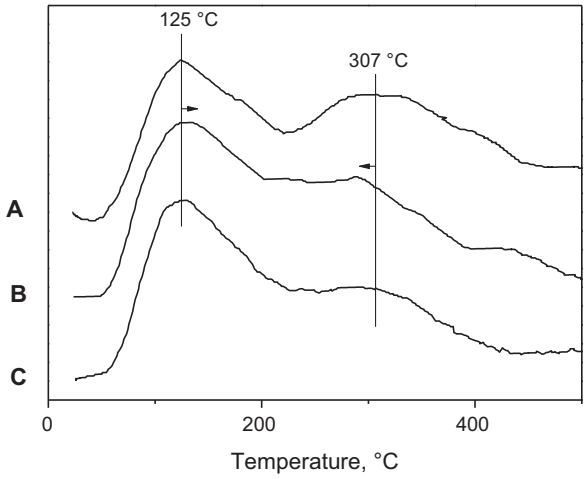

Fig. 5. NH_3-TPD profiles of (A) support CeZr(1), (B) 0.3Au/CeZr(1) and (C) 0.3Pt/CeZr(1).

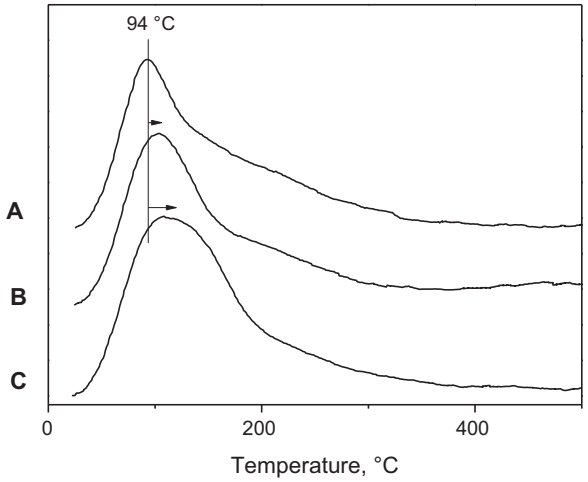

Fig. 6. CO_2-TPD profiles of (A) support CeZr(1), (B) 0.3Au/CeZr(1) and (C) 0.3Pt/CeZr(1).

metal catalysts, again especially for platinum catalyst, points out a higher amount of basic centers in comparison with bare support. TPD characteristics (quantitative data in mmol g^{-1}) of selected catalysts are gathered in Table 2. The overall number of basic sites in the support was 0.135 mmol g^{-1} and increased to 0.395 mmol g^{-1} in the case of platinum catalyst. The NH_3 and CO_2 TPD experiments confirmed that the support is more acidic than basic and that the acidity is decreasing with increasing metal loading (especially for Pt), while the basicity is increasing.

Table 2
TPD characteristics (quantitative data in mmol g^{-1}) of selected catalysts.

	NH_3-TPD (mmol g^{-1})	CO_2-TPD ($mm^3\ g^{-1}$)
CeZr(1)	0.449	0.135
0.3Au/CeZr(1)	0.183	0.201
0.3Pt/CeZr(1)	0.145	0.395

Table 3
Activity and selectivity of selected catalysts in total oxidation of ethanol and toluene.

Catalyst	Ethanol			Toluene		
	T_{50} (°C)	T_{90} (°C)	S_{95} (%)	T_{50} (°C)	T_{90} (°C)	S_{95} (%)
HHC-5557	160	179	86	184	197	100
VOC-1544	172	210	33	153	184	100
0.3Pt/CeZr(1)	167	193	56	187	207	100
2.5Pt/CeZr(1)	99	151	55	167	184	100
2.5Pt/CeZr(2)	116	180	49	172	189	100
0.3Au/CeZr(1)	188	219	88	215	322	100
2.5Au/CeZr(1)	173	210	96	242	281	100
2.5Au/CeZr(2)	190	222	99	255	301	100
CeZr(1)	207	239	95	221	287	100
CeZr(2)	201	246	99	262	363	100

Fig. 7 illustrates four selected FE-SEM images of Au and Pt samples. The particle size distribution, estimated by field-emission scanning electron microscopy confirms the results calculated from XRD patterns.

3.2. Catalytic experiments

Temperatures of 50 and 90% conversion of ethanol and toluene (including selectivity to CO_2) achieved with all catalysts are summarized in Table 3. Comparing the catalysts with 2.5 wt.% loading, platinum-containing samples exhibited higher activity in the oxidation of both ethanol and toluene than their gold analogues. Regardless of the substrate, the activity of these catalysts was decreasing in oxidation of both model compounds in the order:

$$Pt/CeZr(1) > Pt/CeZr(2) > Au/CeZr(1) > Au/CeZr(2)$$

Decreasing the metal loading from 2.5 to 0.3 wt.% led to a lower activity of platinum supported on CeZr(1) in the oxidation of both ethanol and toluene; this decrease was less pronounced in the case of gold catalysts.

The activity of our catalysts was compared to that of industrial ones: VOC-1544 and HHC 5557. In general, all tested catalysts were more active in the oxidation of ethanol than in the oxidation of toluene except VOC-1544. This catalyst, containing 3–6 wt.% Cu + Mn, converted 50% of ethanol at 172 °C and 50% of toluene at 153 °C. There was only 14 °C difference between VOC-1544 and our best catalyst 2.5Pt/CeZr(1) in oxidation of toluene (T_{50} = 167 °C). However, 2.5Pt/CeZr(1) was more efficient catalyst in oxidation of toluene than industrial HHC 5557 containing 0.13 wt.% Pt and 0.04 wt.% Pd (T_{50} = 184 °C). Furthermore, 2.5Pt/CeZr(1) excelled in the oxidation of ethanol where the T_{50} was achieved already at 99 °C (comparing to 50% conversion of ethanol achieved at 160 °C and 172 °C with industrial catalysts HHC 5557 and VOC-1544, respectively).

The differences between activities of tested catalysts in oxidation of ethanol and toluene can be explained by several attributes, which were partly already formulated in similar literature. Baylet et al. published the parametric study of propene oxidation over supported Pt and Au catalysts [54]. The study showed that catalytic activity was not linked to the specific surface area or the metal content but could be attributed to the nature of the metal, the support, to the particle oxidation degree and, to a less extent, the particle

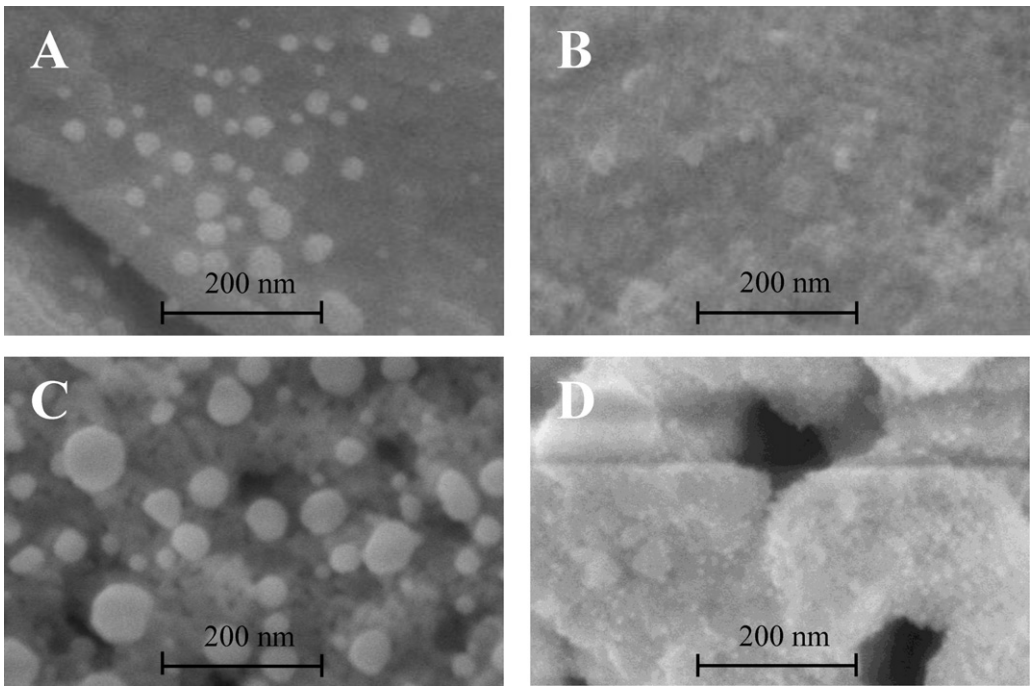

Fig. 7. FE-SEM of (A) 0.3Au/CeZr(1), (B) 0.3Pt/CeZr(1), (C) 2.5Au/CeZr(1) and (D) 2.5Pt/CeZr(1).

size of the metal or the support. Our study confirms that whatever the metal content is, the support impregnated with platinum is always more active than the same support impregnated with gold. Better reductive capability of platinum is confirmed by H_2-TPR profiles (Fig. 4). A higher activity of platinum may be also linked to changes in surface basic properties (a higher amount of basic centers) as illustrated by CO_2-TPD profiles (Fig. 6). Santos et al. [38,57] observed higher activity of Pt than Au in oxidation of ethanol and toluene over TiO_2 supported catalysts as well. Furthermore, specific activities, according to them, depended on O_2 adsorption strengths on metals (volcano plots), and oxidation of ethanol and toluene over supported Pt catalysts was structure sensitive. Metal content influenced catalytic activity of our platinum catalysts but not really the gold ones. This was noticed in spite of the fact, that real metal content of the 2.5 wt.% catalysts was 2.8 wt.% for gold but only 1.5 wt.% for platinum. It may confirm a weak influence of the metal content comparing to the nature of the metal, or to raise a question of optimal amount of noble metal (related to the optimal particle size), which is planned to be studied more precisely in the near future. In our study we experienced the influence of a support as well. CeZr(1), slightly different from CeZr(2) (which is visible e.g. from pore-size distributions, Fig. 3B), showed a little bit better results in oxidation process than CeZr(2). When comparing gold with platinum, another important attribute rising from the characterizations carried out in our study is a presence of Au crystals that are inactive in the oxidation process. Deposition of gold on Ce–Zr mixed oxide resulted in a formation of certain amounts of crystalline Au phase detected by X-ray diffraction while the deposition of platinum did not produce any crystalline Pt phase. This was confirmed by FE-SEM (Fig. 7): while no crystalline Pt phase is visible, it is seen that part of Au is well dispersed but significant amount of Au is present as inactive crystals.

Concerning selectivity, prepared catalysts as well as the industrial ones were more selective in the oxidation of toluene (S_{95} = 100%) than in the oxidation of ethanol (S_{95} from 33 to 99%). Main by-product of the ethanol oxidation was identified as acetaldehyde. With ethanol, the gold catalysts exhibited superior selectivity to the platinum ones; moreover, the selectivity of our gold catalysts was comparable or higher than that of industrial catalysts. Besides others, Maltos and Noronha underlined the influence of the nature of the metal on the product distribution in oxidation of ethanol [38,56]. Their studies revealed that Pt/CeO_2 catalysts show mainly ethoxy species whereas acetate species are mainly formed on Pd/CeO_2 catalyst. The ethoxy species can undergo further dehydrogenation and desorb as acetaldehyde. This could explain the higher selectivity to acetaldehyde observed on supported Pt catalysts. On the other hand, Sheng et al. investigated the reaction of ethanol on the surface of Au/CeO_2 by temperature programmed desorption (TPD), infrared (IR) absorption and in steady-state catalytic conditions [58]. They observed that at 27 °C the surface is covered with both ethoxy species and weakly bonded ethanol. Most of these species desorb giving back ethanol (about 50%; TPD) by 128–177 °C with some formation of acetaldehyde (7.5%; TPD). A small part of the remaining ethoxy gives bridging CO (ν = 1916 cm^{-1}). Most of CO is oxidized to CO_2 ($CO_2/CO \approx 25$; TPD) indicating the powerful nature of Au in the oxidation process. At 327 °C, the surface is covered with carbonates species (ν = 1524 cm^{-1}). As shown by IR and TPD, these carbonates are mainly decomposed to CO_2. Our Pt and Au catalysts are enriched with zirconium and slightly differ from those presented in literature. Nevertheless, we suggest that the influence of the nature of the metal on the product distribution is the main cause of different selectivity of platinum and gold catalysts to acetaldehyde. It is possible that the redox properties of catalysts are a key to more precise explanation of the selectivity to acetaldehyde. Therefore, those properties of platinum and gold catalysts will be studied in the near future.

4. Conclusion

A series of Au and Pt catalysts supported on Ce–Zr mixed oxides, prepared by sol–gel method, was synthesized and tested in total oxidation of toluene and ethanol. The differences between preparation procedure of the CeZr(1) and CeZr(2) support (drying overnight at ambient temperature and drying on sand bath at 60 °C, respec-

tively) slightly altered their pore-size distribution. The CeZr(1) support showed better results in the oxidation of model compounds. Impregnated by noble metals Pt and Au, Ce–Zr mixed oxides showed remarkable activity in the oxidation of toluene and ethanol. Platinum catalysts exhibited higher activity in comparison with corresponding gold catalysts, which can be attributed mainly to the nature of the noble metal. Changes in surface basic properties, optimal metal loading linked to the optimal particle size or presence of inactive Au crystals seems also to play a role in catalytic activity. The efficiency of our platinum catalyst was comparable to that of industrial catalyst, platinum–palladium supported on alumina, even when the metal loading was lower. In the oxidation of ethanol, Au catalysts proved a better selectivity than their platinum analogues already at relatively low metal loading (0.3 wt.%). This is again linked to the nature of the metal, possibly to its influence on redox properties of the catalysts.

Acknowledgements

The financial support from the Grant Agency of the Czech Republic (project nos. P106/10/P019 and P106/11/0902), the Grant Agency of the Academy of Sciences of the Czech Republic (project no. M200720901) and the Ministry of Industry and Trade of the Czech Republic (project no. FR-TI1/059) is greatly appreciated.

References

[1] E.C. Moretti, Practical Solutions for Reducing Volatile Organic Compounds and Hazardous Air Pollutants, American Institute of Chemical Engineers (AIChE), USA, 2001.
[2] F.I. Khan, A.Kr. Ghoshal, J. Loss Prevent. Proc. 13 (2000) 527.
[3] M. Ferrandon, J. Carnö, S. Järås, E. Björnbom, Appl. Catal. B 180 (1999) 153.
[4] P. Papaefthimiaou, T. Ioannides, XE. Verykios, Appl. Catal. B 13 (1997) 175.
[5] J. Mikulová, S. Rossignol, J. BarbierJr., D. Mesnard, C. Kappenstein, D. Duprez, Appl. Catal. B 72 (2007) 1.
[6] J.J. Spivey, Ind. Eng. Chem. Res. 26 (1987) 2165.
[7] N. Radic, B. Grbic, A. Terlecki-Baricevic, Appl. Catal. B 50 (2004) 153.
[8] K. Kim, H. Ahn, Appl. Catal. B 91 (2009) 308.
[9] B. Grbic, N. Radic, A. Terlecki-Baricevic, Appl. Catal. B 50 (2004) 161.
[10] K. Kim, S. Boo, H. Ahn, J. Ind. Eng. Chem. 15 (2009) 92.
[11] T. Masui, H. Imadzu, N. Matsuyama, N. Imanaka, J. Hazard. Mater. 176 (2010) 1106.
[12] A.A. Barresi, M. Cittadini, A. Zucca, Appl. Catal. B 43 (2003) 27.
[13] A.C.C. Rodrigues, Catal. Commun. 8 (2007) 1227.
[14] G. Colon, M. Maicu, M.C. Hidalgo, J.A. Navio, A. Kubacka, M. Fernandez-Garcia, J. Mol. Catal. A 320 (2010) 14.
[15] S. Ordonez, L. Bello, H. Sastre, R. Rosal, F.V. Diez, Appl. Catal. B 38 (2002) 139.
[16] C. Young, T.M. Lim, K. Chiang, J. Scott, R. Amal, Appl. Catal. B 78 (2008) 1.
[17] T. Sano, N. Negishi, K. Takeuchi, S. Matsuzawa, Sol. Energy 77 (2004) 543.
[18] Y. Ma, M. Chen, C. Song, X. Zheng, Acta Phys.: Chim. Sinica 24 (2008) 1132.
[19] J.C. Wu, T. Chang, Catal. Today 44 (1998) 111.
[20] N. Burgos, M. Paulis, J. Sambeth, J.A. Odriozola, M. Montes, Stud. Surf. Sci. Catal. 118 (1998) 157.
[21] M. Paulis, H. Peyrard, M. Montes, J. Catal. 199 (2001) 30.
[22] H. Song, X. Qiu, X. Li, F. Li, W. Zhu, L. Chen, J. Power Sources 170 (2007) 50.
[23] R.T.S. Oliveira, M.C. Santos, B.G. Marcussi, S.T. Tanimoto, L.O.S. Bulhoes, E.C. Pereira, J. Power Sources 157 (2006) 212.
[24] J.M. Sieben, M.M.E. Duarte, Int. J. Hydrogen Energy 36 (2011) 3313.
[25] J.C.M. Silva, R.F.B. De Souza, L.S. Parreira, E. Teixeira Neto, M.L. Calegaro, M.C. Santos, Appl. Catal. B 99 (2010) 265.
[26] E. Higuchi, K. Miyata, T. Takase, H. Inoue, J. Power Sources 196 (2011) 1730.
[27] S.S. Mahapatra, A. Dutta, J. Datta, Electrochim. Acta 55 (2010) 9097.
[28] F.H.B. Lima, E.R. Gonzalez, Appl. Catal. B 79 (2008) 341.
[29] D.R.M. Godoi, J. Perez, H.M. Villullas, J. Power Sources 195 (2010) 3394.
[30] H. Wang, Z. Jusys, R.J. Behm, J. Power Sources 154 (2006) 351.
[31] X. Tang, B. Zhang, Y. Li, Y. Xu, Q. Xin, W. Shen, J. Mol. Catal. A 235 (2005) 122.
[32] L. Colmenares, H. Wang, Z. Jusys, L. Jiang, S. Yan, G.Q. Sun, R.J. Behm, Electrochim. Acta 52 (2006) 221.
[33] F. Kadirgan, S. Beyhan, T. Atilan, Int. J. Hydrogen Energy 34 (2009) 4312.
[34] S. Strbac, M. Avramov Ivic, Electrochim. Acta 54 (2009) 5408.
[35] F. Cheng, X. Dai, H. Wang, S.P. Jiang, M. Zhang, C. Xu, Electrochim. Acta 55 (2010) 2295.
[36] Q. He, W. Chen, S. Mukerjee, S. Chen, F. Laufek, J. Power Sources 187 (2009) 298.
[37] M. Ousmane, L.F. Liotta, G. Di Carlo, G. Pantaleo, A.M. Venezia, G. Deganello, L. Retailleau, A. Boreave, A. Giroir-Fendler, Appl. Catal. B 101 (2011) 629.
[38] V.P. Santos, S.A.C. Carabineiro, P.B. Tavares, M.F.R. Pereira, J.J.M. Orfao, J.L. Figueiredo, Appl. Catal. B 99 (2010) 198.
[39] M. Hosseini, S. Siffert, R. Cousin, A. Aboukais, Z. Hadj-Sadok, B. Su, C.R. Chem. 12 (2009) 654.
[40] N. Dimitratos, A. Villa, D. Wang, F. Porta, D. Su, L. Prati, J. Catal. 244 (2006) 113.
[41] H.L. Tidahy, T. Barakat, R. Cousin, C. Gennequin, V. Idakiev, T. Tabakova, Z. Yuan, B. Su, S. Siffert, Stud. Surf. Sci. Catal. 175 (2010) 743.
[42] S.J. Schmieg, D.N. Belton, Appl. Catal. B 6 (1995) 127.
[43] M. Thammachart, V. Meeyo, T. Risksomboon, S. Osuwann, Catal. Today 68 (2001) 53.
[44] A. Cabana, J.A. Darr, E. Lester, M. Poliakoff, J. Mater. Chem. 11 (2001) 561.
[45] E. Rohart, O. Larcher, C. Heĭdouin, M. Allain, P. Macaudieĭ re, SAE Int. Pape 1, 2001, p. 1274.
[46] A. Trovarelli, Structural properties and nonstoichiometric behavior of CeO_2, in: A. Trovarelli (Ed.), Catalysis by Ceria and Related Materials, Catalysis Science Series, Imperial College Press, 2002, p. 2.
[47] A. Trovarelli, Catal. Rev. Sci. Eng. 38 (1996) 439.
[48] J. Kaspar, P. Fornasiero, M. Graziani, Catal. Today 50 (1999) 285.
[49] J.I. Gutiérrez-Ortiz, B. Rivas, R. López-Fonseca, J.R. González-Velasco, Appl. Catal. B 65 (2006) 191.
[50] B. de Rivas, R. Lopez-Fonseca, C. Sampedro, J.I. Gutierez-Ortiz, Appl. Catal. B 90 (2009) 545.
[51] S. Azalim, R. Brahmi, M. Bensitel, J. Giraudon, J. Lamonier, Stud. Surf. Sci. Catal. 175 (2010) 731.
[52] Z.M. Liu, J.L. Wang, J.B. Zhong, Y.Q. Chen, S.H. Yan, M.C. Gong, J. Hazard. Mater. 149 (2007) 742.
[53] D. Terribile, A. Trovarelli, C. Leitenburg, A. Primavera, G. Dolcetti, Catal. Today 47 (1999) 133.
[54] A. Baylet, C. Capdeillayre, L. Retailleau, J.L. Valverde, P. Vernoux, A. Giroir-Fendler, Appl. Catal. B 102 (2011) 180.
[56] L.V. Mattos, F.B. Noronha, J. Power Sources 152 (2005) 50.
[57] A.M. Silva, L.O.O. Costa, A.P.M.G. Barandas, L.E.P. Borges, L.V. Mattos, F.B. Noronha, Catal. Today 133–135 (2008) 755.
[58] P.Y. Sheng, G.A. Bowmaker, H. Idriss, Appl. Catal. A 261 (2004) 171.